Made available by Hasselt University Library in https://documentserver.uhasselt.be

A detailed investigation of the microwave assisted phenylphosphonic acid modification of P25 TiO2

Peer-reviewed author version

TASSI, Marco; Roevens, Annelore; REEKMANS, Gunter; VANHAMEL, Martine; Meynen, Vera; D'HAEN, Jan; ADRIAENSENS, Peter & CARLEER, Robert (2017) A detailed investigation of the microwave assisted phenylphosphonic acid modification of P25 TiO2. In: ADVANCED POWDER TECHNOLOGY, 28(1), p. 236-243.

DOI: 10.1016/j.apt.2016.09.020
Handle: http://hdl.handle.net/1942/24153

A detailed investigation of the microwave assisted phenylphosphonic acid modification of P25 TiO_2

Marco Tassi[1], *Annelore Roevens*[2], *Gunter Reekmans*[1], *Martine Vanhamel*[1], *Vera Meynen*[2], *Jan D'Haen*[1], *Peter Adriaensens*[1], *Robert Carleer*[1]

1-Applied and Analytical Chemistry, Institute for Materials Research (IMO), Hasselt University, Agoralaan 1 - Building D, B-3590 Diepenbeek, Belgium

2-Laboratory of Adsorption and Catalysis, University of Antwerp, Universiteitsplein 1, B-2610 Wilrijk, Belgium.

KEYWORDS: TiO_2 surface modification, titaniumphenylphosphonate, ATR-FTIR, ^{31}P solid state NMR, TEM, phosphonic acid

ABSTRACT: The microwave assisted reaction between P25 titanium dioxide (TiO_2) and phenylphosphonic acid (PPA) is explored thoroughly and the influence of the reaction conditions on the grafting mechanism and formed products is presented. While the surface grafting is observed at low temperatures and water free conditions, the formation of titaniumphosphonate is favored in water and high reaction temperatures. For the first time the correlation between the amorphous TiO_2 phase and the formation of titaniumphenylphosphonate is reported. Materials are fully characterized by attenuated total reflectance-Fourier transform infrared spectroscopy (ATR-FTIR), solid-state ^{31}P Nuclear Magnetic Resonance (^{31}P-NMR) spectroscopy, energy dispersive X-ray (EDX) spectroscopy and transmission electron microscopy (TEM).

INTRODUCTION

In various innovative applications, the material performance depends on the physico-chemical properties of the surface, explaining the broad interest in organic surface modifications[1,2,3,4,5]. Transition metal oxides are gaining much interest because of their intrinsic chemical and corrosive stability in a wide variety of solvents and pH-ranges[3,6,7,8]. One of the most studied metal oxides is Aeroxide P25 titanium dioxide, produced via the Aerosil® process[9], and being used as de-facto standard titanium photocatalyst in the last twenty years[10]. In this process, the titanium tetrachloride ($TiCl_4$) precursor is hydrolyzed in the vapor phase at 985°C in a H_2/O_2 flame, resulting in the formation of primary particles with an average size of 21 nm[9]. In 1999, Porter et al described the P25 composition as 76.5% anatase and 23.5% rutile, but also revealed that it was possible to increase the rutile content via calcination in the temperature range 600°C-1000°C[11]. In 2006, Jensen et al reported that P25 was composed of 71% anatase, 27% rutile and 2% amorphous phase[12]. The presence of an amorphous phase was also mentioned before in 2001 by Ohno[9]. Ohtani et al[13] reported a variable P25 composition varying between 73%-85% anatase, 14-17% rutile and 0-13% amorphous TiO_2. Although the composition of the TiO_2 P25 in terms of anatase/rutile/amorphous ratio has been intensively investigated, the conclusions were not consistent[11,12,13], until advanced X Ray quantification was performed by Tobaldi et al. in 2014 from which it was established that TiO_2 P25 is composed of 76.3% anatase, 10.6% rutile and 13.0% amorphous phase[14]. In the last 25 years increasing attention has been paid on the modification of titanium dioxide with alkyl- or phenyl-substituted phosphonic acids [15,16,17,18,19]. P25 TiO_2 modifications with phosphonic acids have been investigated in order to modify the properties of the nanosized crystallite surfaces[15,17,20,21]. The coupling of the organophosphorous compounds to the P25 surface is reported to occur via stable covalent Ti-O-P bonds formed via a heterocondensation reaction between the phosphonic acid and the P25 surface hydroxyl groups[20,21,22]. According to literature, this heterocondensation consists of two major steps: (1) the protonation of the surface hydroxyl group and (2) the nucleophilic attack by the phosphonic acid and simultaneous release of water[22]. Different binding modes, differentiated

by the number of Ti-O-P bonds involved, have been individuated[15,20,21]. In general, one differentiates between the monodentate, bidentate and tridentate binding mode[15,20,21,23]. Whereas the bidentate mode results from the heterocondensation of the two P-OH groups with surface hydroxyl groups, the formation of tridentate structures is stated to involve the P=O group[21] but the mechanism is still not clear from literature. The techniques most frequently used to investigate the resulting chemical structures and binding modes are ATR-FTIR and solid state (SS) ^{31}P-NMR spectroscopy. ATR-FTIR is suitable since it provides information regarding the P-O, P=O and P-C bonds via absorbances in the 900-1400 cm^{-1} region[15,21,22,24]. ^{31}P NMR is useful to distinguish between grafted phosphonic acid species and titaniumphosphonate[24]. The latter species are described to be the result of a dissolution-precipitation mechanism resulting from partial hydrolysis of the TiO_2 matrix[17,20,22,24]. However, there is still a lack of experimental evidences for the proposed mechanism. Several studies reported that covalent coupling of phenylphosphonic acid to TiO_2 results in a broad signal shifted upfield by about 9 ppm as compared to the chemical shift of the free phenylphosphonic acid around 21 ppm[14,16,21,22,24,25]. ^{31}P-NMR spectra of samples obtained by reacting TiO_2 with PPA at high temperatures (≥ 100°C) also showed an isolated resonance signal at -4 ppm, i.e. shifted upfield by about 25 ppm as compared to free phenylphosphonic acid[22,24]. Studies[16,26,27,28] on the reaction product of $TiCl_4$ or titanium tetraisopropoxide with phenylphosphonic acid revealed a similar signal which was assigned to the phosphorus atoms of the α-titanium phenylphosphonate phase formed by dissolution-precipitation of the matrix[22,24,29]. Guerrero et al concluded that it is possible to form a mixture of monodentate, bidentate and tridentate structures at the surface through heterocondensation under mild reaction conditions while Ti-O-Ti bond cleavage can occur preferably at more severe reaction conditions (i.e. 24h at 100°C).[20,22,29]. Despite the high amount of literature available, the modification of P25 TiO_2 presents still knowledge gaps that has to be fulfilled. Especially the influence of the reaction conditions and the crystal-amorphous phases of P25 on the modification process requires an in depth investigation. In this work the effect of reaction conditions is studied using a microwave

assisted modification which can be considered as a novelty in the field of metal oxide functionalization. The obtained structures are characterized using advanced and complementary techniques such as SS ^{31}P-NMR, ATR-IR, EDX spectroscopy and TEM microscopy. Additionally, this paper aims also to understand the impact of crystal-amorphous phases on the modification of P25 with PPA. Finally, this work aims to define the key parameters for the monitoring of P25 modifications which will have a direct effect on its application.

EXPERIMENTAL SECTION

Hydrophilic fumed P25 TiO_2 powder (Aeroxide), with a specific surface area of 50 m^2/g and an average primary particle size of 21 nm was used as substrate material. Phenylphosphonic acid ($PhPO_3H_2$, PPA, 98%, 158.09 MW) was obtained from Aldrich, analyzed for structure and purity by SS ^{31}P-NMR and used without further purification. For the synthesis of **TiO_2/PPA-20°C**, 1 g of TiO_2 was dispersed in 20 ml of a 0.1 M solution of PPA in MilliQ water (316 mg/20 ml). After stirring the reaction mixture for 24 h at 20°C, the solid was recovered by membrane filtration (VitraPOR Borosilicate 3.3) and washed with 200 ml MilliQ water in order to remove remaining free PPA. Finally the material was dried at 120°C under vacuum for 24h[20,22]. Synthesis of the series of **TiO_2/PPA-xx°C** materials was accomplished as for TiO_2/PPA-20°C but by reacting for 3h in a microwave (MW) reactor (CEM Explorer) at 45°C (TiO_2/PPA-45°C), 60°C (TiO_2/PPA-60°C), 75°C (TiO_2/PPA-75°C), 90°C (TiO_2/PPA-90°C), 105°C (TiO_2/PPA-105°C), 120°C (TiO_2/PPA-120°C) and 150°C (TiO_2/PPA-150°C). Table 1 shows the experimental conditions regarding the microwave assisted reactions. The resulting materials were recovered, washed and dried as described above. For the preparation of **TiO_2 thermally treated at 600°C and 1000°C**, 1 gram of TiO_2 powder was treated for 6 hours in a muffle furnace at 600°C or 1000°C. Hereafter, the powder was treated with PPA as described above for the TiO_2/PPA-xx°C materials.

Table 1 Experimental conditions of the microwave assisted reactions.

Material	Maximum temperature before set point(°C)	Maximum pressure before set point (PSI)	Time to obtain the set point (s)	Average temperature during 3h reaction (°C)	Average pressure during 3h reaction (PSI)	Average power during 3h reaction (W)
TiO_2/PPA-45°C	51	2	27	45	0	7
TiO_2/PPA-60°C	85	33	89	60	0	15
TiO_2/PPA-75°C	80	45	60	75	0	15
TiO_2/PPA-90°C	113	58	121	90	0	20
TiO_2/PPA-105°C	124	61	126	105	0	30
TiO_2/PPA-120°C	141	117	142	120	35	35
TiO_2/PPA-150°C	154	203	225	150	100	45
TiO_2/PPA-90°C acetone	97	91	112	90	50	25

The resulting materials were recovered, washed and dried as described above. **Preparation of TiO_2/PPA-90°C-acetone**. Hereto, 1 g of TiO_2 was dispersed in 20 ml of a 0.1 M solution of PPA in acetone. After stirring the reaction mixture for 3 h at 90°C in the microwave reactor, the solid material was recovered, washed and dried as described above. **ATR-FTIR (attenuated total reflectance-Fourier transform infrared)** spectra were obtained at a resolution of 4 cm^{-1} with 64 scans on a Bruker Vertex 70 spectrometer equipped with a DTGS detector and a PIKE MIRacle ATR unit with a diamond crystal. Solid-state **^{31}P-CP/MAS** (cross-polarization/magic angle spinning) **NMR** spectra were acquired at ambient temperature on an Agilent VNMRS DirectDrive 400MHz spectrometer (9.4 T wide bore magnet) equipped with a T3HX 3.2 mm probe dedicated for small sample volumes and high decoupling powers. Magic angle spinning (MAS) was performed at 10 kHz using ceramic zirconia rotors of 3.2 mm in diameter (22 µl rotors) and with TOSS (total suppression of spinning sidebands). The phosphorus chemical shift scale was calibrated

towards orthophosphoric acid (H_3PO_4) at 0 ppm. Other acquisition parameters used were: a spectral width of 50 kHz, a 90° pulse length of 2.5 μs, a spin-lock field for CP of 100 kHz, a contact time for CP of 1.7 ms, an acquisition time of 20 ms, a recycle delay time of 20 s and 200-3000 accumulations. High power proton dipolar decoupling during the acquisition time was set at 100 kHz. The Hartmann-Hahn condition for CP was calibrated accurately on the samples themselves. **Transmission electron microscopy (TEM)** was accomplished with a Tecnai Spirit TEM operating at 120 kV in order to study the morphology and crystal structure of the powders. The local element composition is determined with energy dispersive X-ray (**EDX**) analysis (Si(Li)detector). **Quantification of the amount of water generated during the synthesis of TiO_2/PPA-90°C-acetone.** Hereto, the filtrate of the post-reaction mixture was analyzed by means of a Karl Fisher titration, with the 0.1 M solution of PPA in acetone as a reference.

RESULTS AND DISCUSSION

In this study, P25 TiO_2, was modified with phenylphosphonic acid (PPA) in a microwave reactor. The microwave assisted synthesis of TiO_2 based materials was experimented because it was expected that this technology would be more efficient as compared to conventional heating methods[30,31,32]. The use of a microwave reactor allows the selective heating of the reactants without heating the entire furnace or oil bath, reducing reaction time and energy. Moreover, a uniform distribution of the heat is assured and several examples of higher yields are reported[33]. Another important advantage is the superheating of the solvent, allowing to perform reactions highly above the boiling point of the solvent used. Since physically adsorbed PPA can be removed during the reaction work-up (filtration and washing), only PPA which is covalently bonded to the surface of the TiO_2 nanosized crystals is considered as a stable metal oxide modification. **Figure 1** shows a series of ATR-FTIR spectra of TiO_2 based materials obtained after modification with PPA as a function of the reaction temperature. The TiO_2/PPA-20°C material (**Figure 1A**) is characterized by

the presence of IR absorbances at 3065, 1439 and 1154 cm^{-1}, being assigned to respectively the aromatic C-H, C=C and P-C stretch vibrations of PPA[22,34]. The ^{31}P-NMR spectrum of TiO_2/PPA-20°C (**Figure 2B**) shows a broad resonance signal between 2-25 ppm, being a superposition of resonances. According to literature these are resulting from monodentate, bidentate and tridentate binding modes[22,24]. However other literature studies[23,35,36] described the geometry of the tridentate binding mode as highly unfavorable. The broadening of the signal is the result of multiple, slightly different geometries due to multiple non-covalent physico-chemical interactions (e.g hydrogen bonds) involved via the P-OH and P=O groups[21]. Remark that the water released during the heterocondensation reaction is negligible with respect to the water present as reaction solvent. Quantification of the amount of water generated during the formation of P-O-Ti bonds was carried out by means of Karl Fisher titration resulting inconclusive.

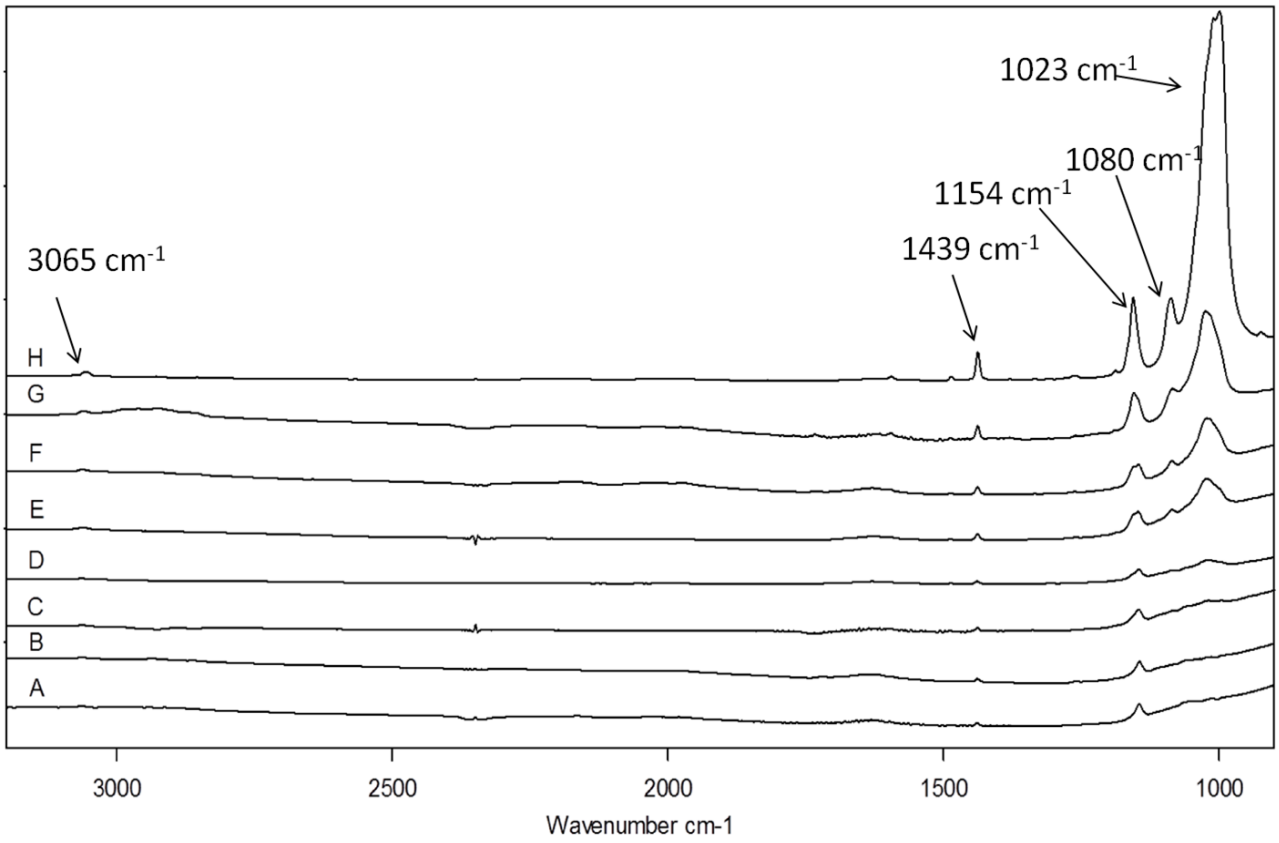

Figure 1: ATR-FTIR spectra of TiO_2 modified with a 0.1 M solution of phenylphosphonic acid (PPA) in water. A) TiO_2/PPA-20°C, B) TiO_2/PPA-45°C, C) TiO_2/PPA-60°C, D) TiO_2/PPA-75°C, E) TiO_2/PPA-90°C, F) TiO_2/PPA-105°C, G) TiO_2/PPA-120°C, H) TiO_2/PPA-150°C.

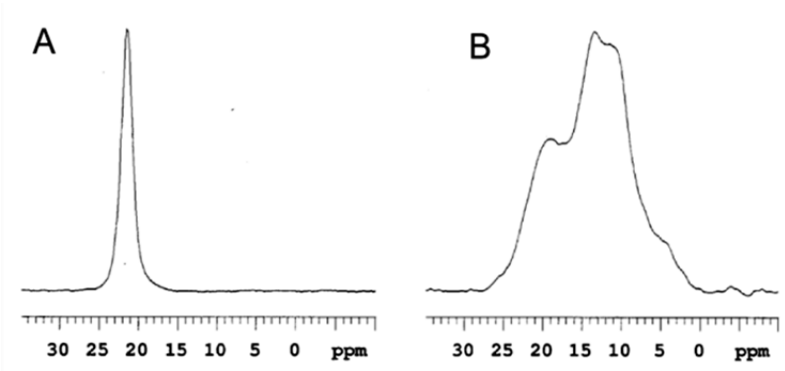

Figure 2: ^{31}P-CP/MAS NMR spectra of A) PPA and B) TiO_2/PPA-20°C.

The TEM micrograph of TiO_2/PPA-20°C (Figure 3A) only shows nanocrystallites as for pure TiO_2 P25 (Figure 3B), demonstrating the absence of new structures. This in contrast to TiO_2/PPA-150°C (see Figure 7) in which new titaniumphenylphosphonate structures are formed. The EDX spectrum of these nanocrystallites (Figure 4) reveals minor amounts of phosphorous and carbon confirming that TiO_2/PPA-20°C is composed of nanosized TiO_2 crystals modified with PPA.

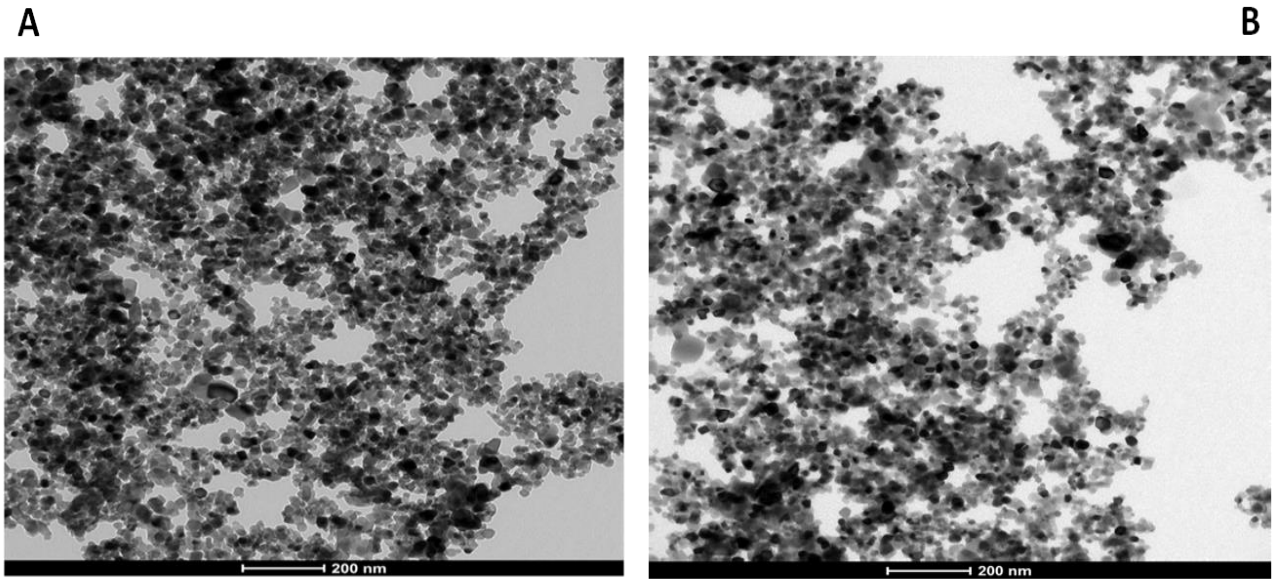

Figure 3: TEM images of A)TiO_2/PPA-20°C and B) pure TiO_2 P25 nanopowder.

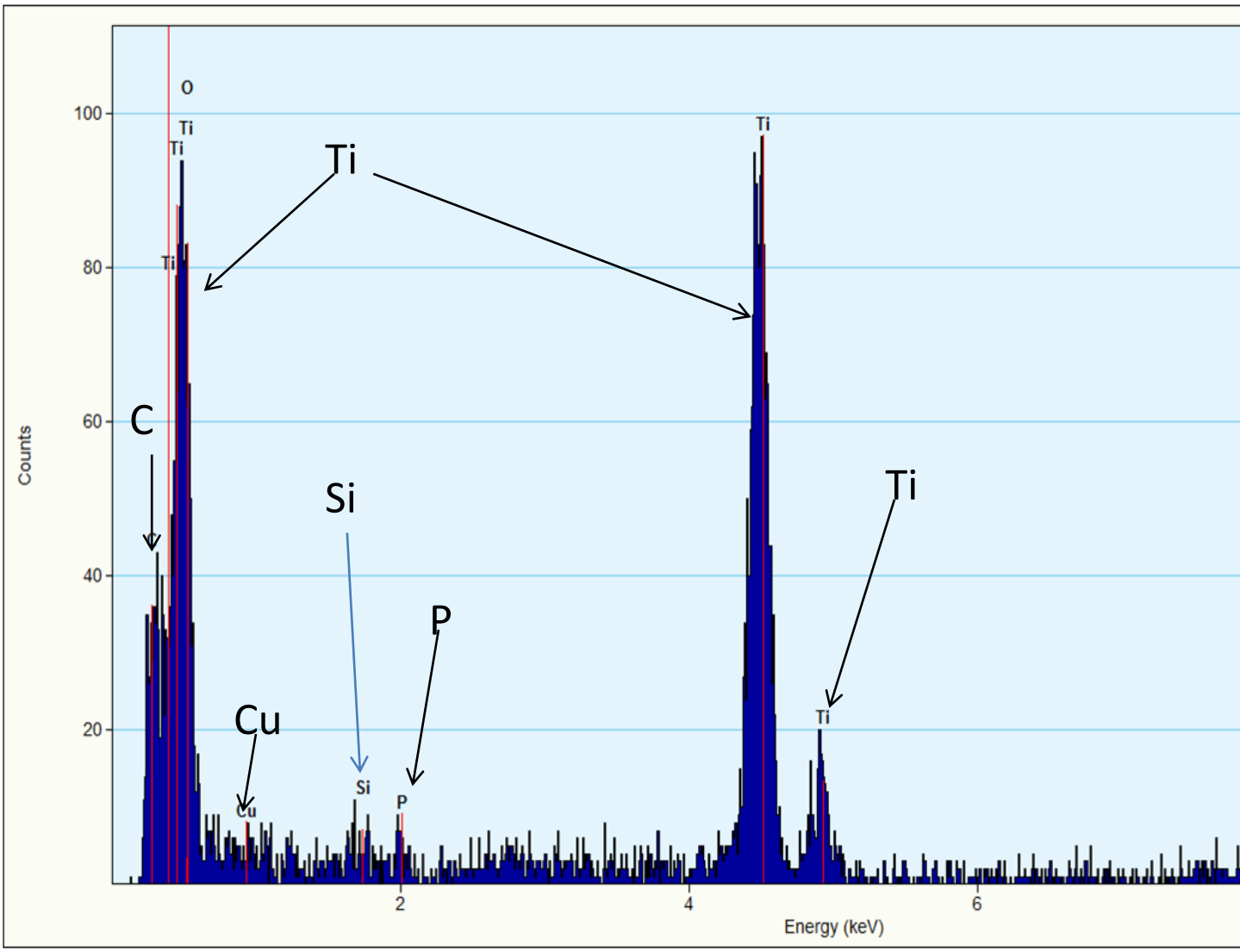

Figure 4: EDX analysis of TiO_2/PPA-20°C.

While the ATR-FTIR spectra of TiO_2/PPA-20°C and TiO_2/PPA-45°C (Figure 1B) are similar, the ^{31}P-NMR spectrum of TiO_2/PPA-45°C (Figure 5A) reveals the appearance of a new signal at -4 ppm arising from titaniumphenylphosphonate. This apparent lack of agreement is due to the broad TiO_2 absorption band at lower wavenumber, preventing the detection of new signals at an early stage in the spectral region between 1000 and 1100 cm^{-1} (see later). The ATR-FTIR spectra of TiO_2/PPA-60°C and TiO_2/PPA-75°C (Figure 1C-D) starts to display the appearance of new absorbances around 1080 cm^{-1} and 1023 cm^{-1} which can be assigned to the asymmetrical and symmetrical stretching vibrations of the $–P(O–Ti)_3$ functionalities of titaniumphosphonate structures[28].

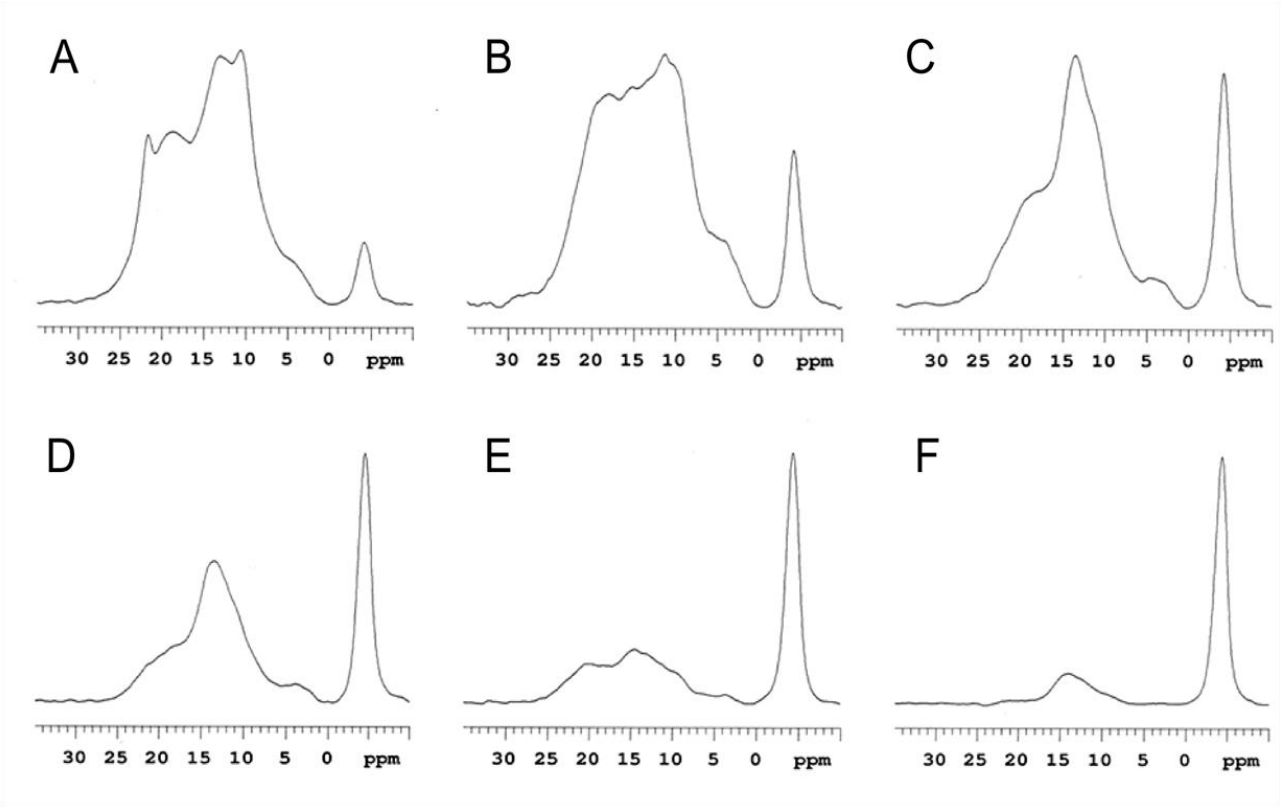

Figure 5: ^{31}P-CP/MAS NMR spectra of TiO_2 after reacting with a 0.1 M solution of phenylphosphonic acid (PPA) in water for 3 hours. A) TiO_2/PPA-45°C, B) TiO_2/PPA-60°C, C) TiO_2/PPA-75°C, D) TiO_2/PPA-90°C, E) TiO_2/PPA-105°C and F) TiO_2/PPA-120°C.

The ATR-FTIR spectra of TiO_2/PPA-90°C, TiO_2/PPA-105°C, TiO_2/PPA-120°C and TiO_2/PPA-150°C (Figures 1E-H) show that an increase in reaction temperature is correlated with an intensity increase of these absorbances around 1023 and 1080 cm^{-1}. Moreover, a significant increase of the phenyl ring related PPA absorptions (3065, 1439 and 1154 cm^{-1}) is observed for reactions at increasing temperatures, pointing to an increase of PPA modification. Regarding the ^{31}P-NMR spectra, a relative increase of the downfield part of the broad band between 2-25 ppm is observed upon increasing the reaction temperature to 60°C (Figure 5B).

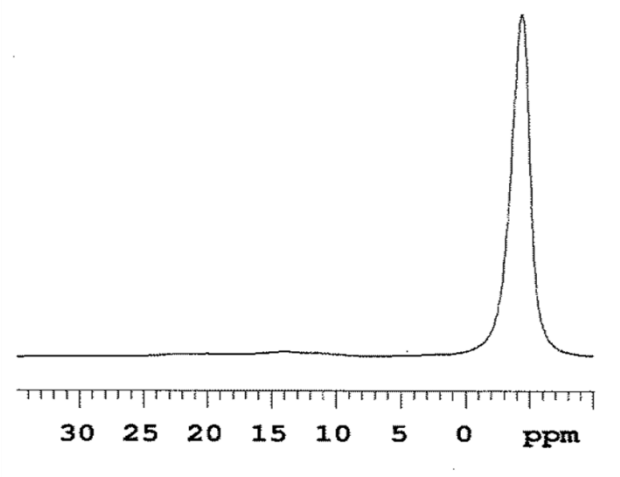

Figure 6: ^{31}P-CP/MAS NMR spectrum of TiO_2 after reacting with a 0.1 M solution of phenylphosphonic acid (PPA) in water at 150°C (TiO_2/PPA-150°C).

Further elevation of the reaction temperature however results in a relative increase of the upfield part of this band (Figure 5C-F). Starting from a reaction temperature of around 90°C, the signal at -4 ppm becomes more dominant as shown in the ^{31}P-NMR spectra of TiO_2/PPA-105°C and TiO_2/PPA-120°C (Figure 5E-F). Figure 6 shows the ^{31}P-NMR spectrum of TiO_2/PPA-150°C in which almost only the signal of the titaniumphenylphosphonate is observed. The broad signal between 2-25 ppm, arising from monodentate and bidentate bonded PPA, is only observed after expanding the vertical scale strongly (supporting information 1). Moreover, it has to be noted that the titaniumphenylphosphonate formation takes place much faster in the microwave reactor as compared to classical synthesis set-ups using conventional heating methods[22,26].

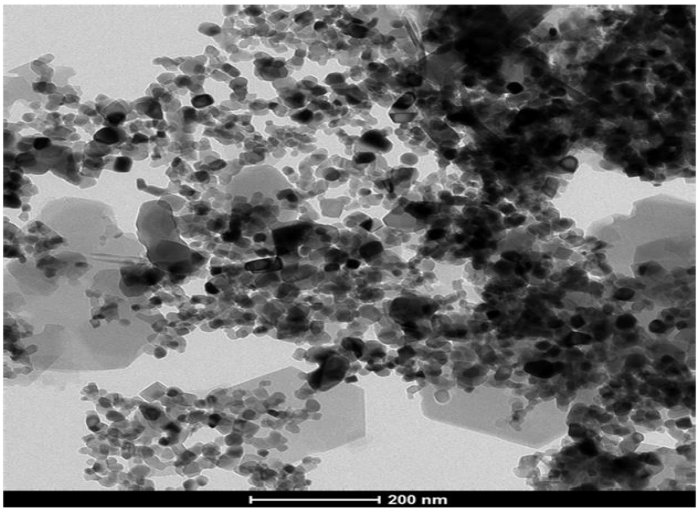

Figure 7: TEM image of TiO_2/PPA-150°C.

The TEM image of TiO_2/PPA-150°C (Figure 7) clearly shows the presence of TiO_2 nanocrystallites coexisting with 150-200 nm agglomerates of titaniumphenylphosphonate. The EDX spectrum obtained by focusing on the agglomerates shows a high C/Ti as well as P/Ti ratio (Figure 8) originating from the titaniumphenylphosphonate structure in which each Ti is surrounded by two P atoms and twelve C atoms per unit of $Ti(C_6H_5PO_3)_2$ (supporting information 2).

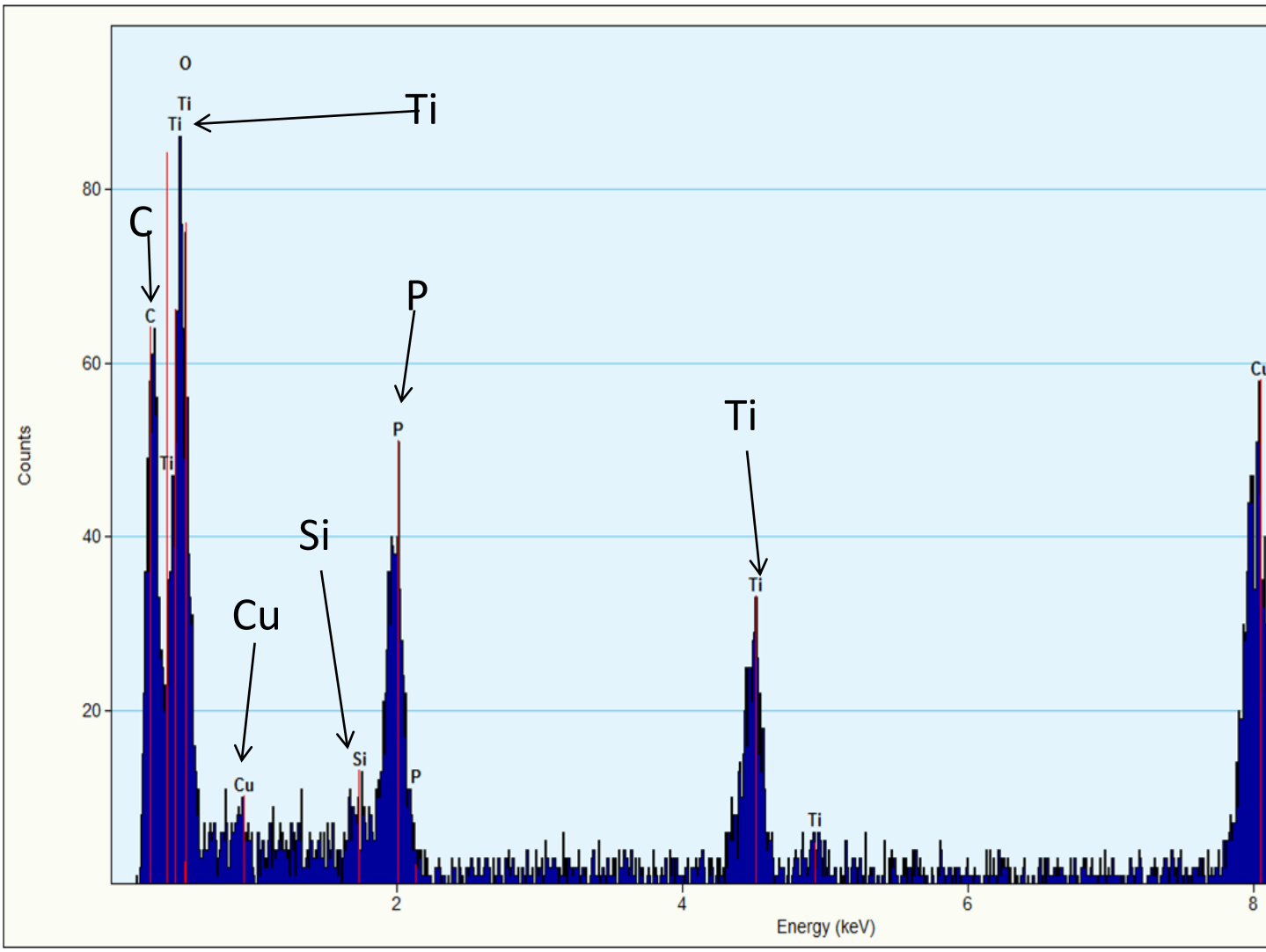

Figure 8: EDX analysis of titaniumphenylphosphonate in TiO_2/PPA-150°C.

Figure 9 presents a high resolution TEM image of TiO_2/PPA-150°C showing that the titaniumphenylphosphonate aggregates consist of lamellae with an interlayer distance of 16 Å. Such a layered structure is similar to the zirconiumphosphonate structure mentioned by Clearfield and

Alberti[37,38,39,40]. EDX analysis with focus on the nanocrystallites (Figure 10) shows a much smaller C/Ti and P/Ti ratio, indicative for a nanocrystal surface grafting with PPA.

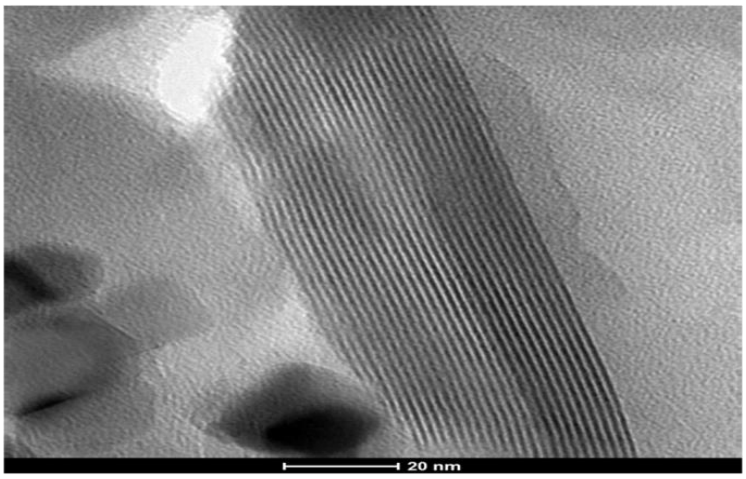

Figure 9: TEM image of TiO_2/PPA-150°C showing the lamellar structure of the titaniumphenylphosphonate aggregates.

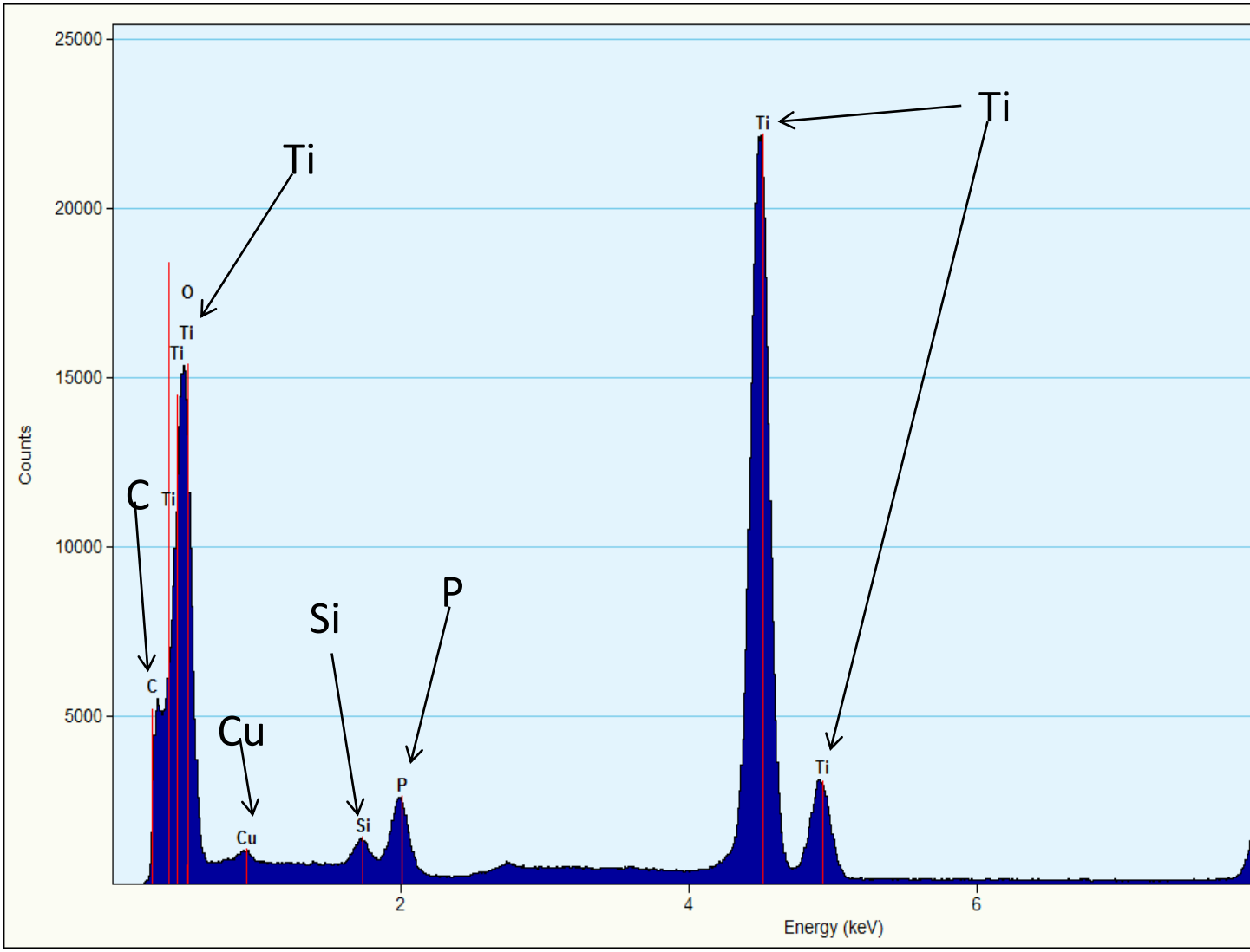

Figure 10: EDX analysis of the nanocrystals of TiO_2/PPA-150°C.

The presence of water seems to be essential for the formation of titaniumphenylphosphonate. This could be demonstrated by performing a microwave reaction between TiO_2 and PPA at 90°C in dried acetone. This modification resulted in a reaction product showing two signals in the ^{31}P-NMR spectrum (Figure 11). The sharp resonance at 21 ppm can be attributed to remaining physically adsorbed PPA which was not removed by the washing step. The broad signal between 2-25 ppm can be attributed to PPA which is covalently bonded at the surface of the TiO_2 nanocrystals. The almost complete absence of the signal at -4 ppm indicates that the formation of titaniumphenylphosphonate is strongly suppressed. As a conclusion, it can be stated that water plays an essential role in the formation of titaniumphenylphosphonate, most probably in supporting the hydrolysis of the Ti-O-Ti bonds, a cleavage also described by Guerrero[22,29].

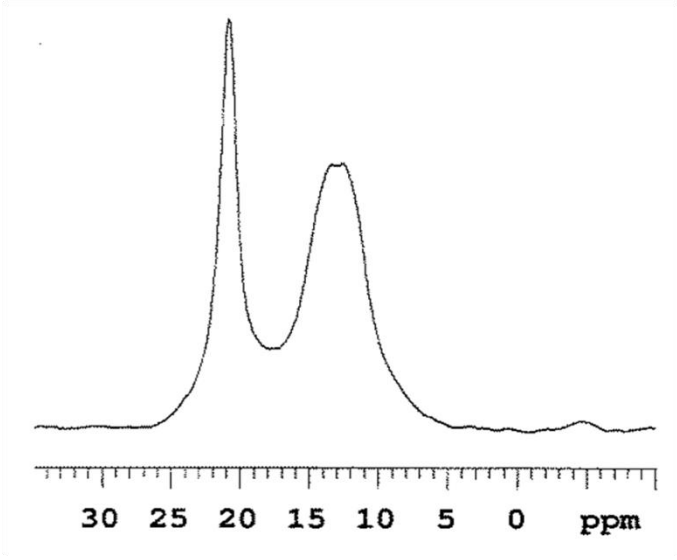

Figure 11: ^{31}P-CP/MAS NMR spectrum of TiO_2/PPA-90°C- acetone.

The subsequent self-assembly of $Ti(C_6H_5PO_3)_2$ units into the final titaniumphenylphosphonate crystalline structure is confirmed by the TEM images shown in Figures 7 and 9. In addition to the reaction conditions (temperature and solvent) the substrate was investigated in more detail too. Hereto the effect of calcination on the reactivity of P25 was studied by thermal pre-treatments of 6 hours at respectively 600 °C and 1000°C prior to reaction with PPA in water at 150°C in the microwave reactor. A thermal pre-treatment at 600°C only causes the crystallization of amorphous

TiO_2 into anatase[11]. Neither a transition from anatase to rutile nor a significant increase in primary particle size was reported for such treatment[11,41]. Figure 12 shows ATR-FTIR spectra illustrating the effect of both thermal pre-treatments on the microwave reaction of TiO_2 with PPA in water at 150°C. The peak area of the absorption band around 1023 cm^{-1} was used as a measure to evaluate the relative amount of titaniumphosphonate. The spectrum of 600°C pre-treated TiO_2 after reaction with PPA at 150°C (Figure 12A) shows that the peak area is significantly reduced as compared to this of TiO_2/PPA-150°C shown in figure 1H. The reduction of titaniumphenylphosphonate is also confirmed by ^{31}P-NMR analysis (supporting information 3). These results indicate that a decreasing amount of amorphous TiO_2 affects the amount of titaniumphenylphosphonate formed[11] and allows to presume a direct correlation between the amorphous TiO_2 content and the formation of titaniumphenylphosphonate.

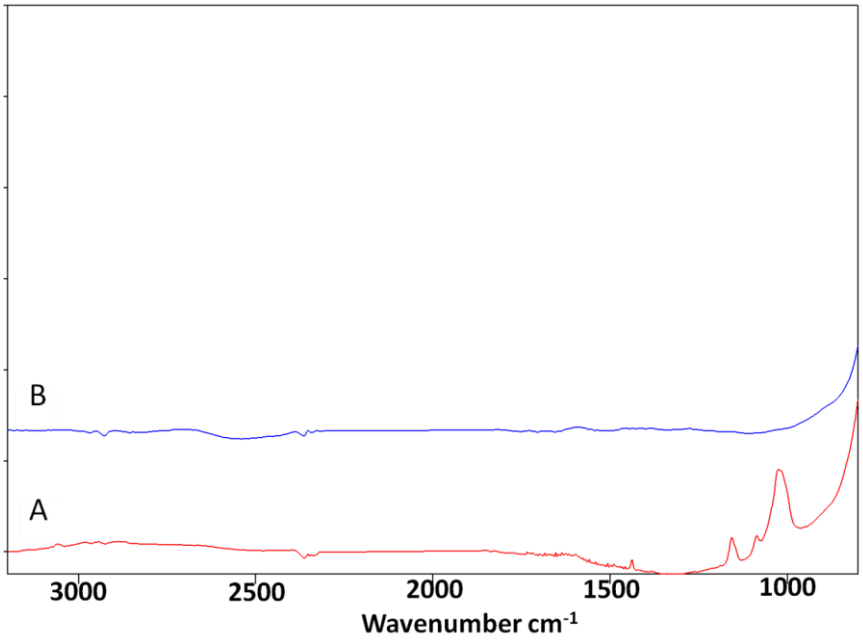

Figure 12 : ATR-IR of A) TiO_2 after a thermal pre-treatment at 600°C followed by reaction with PPA at 150°C in MW and B) TiO_2 after a thermal pre-treatment at 1000 °C followed by reaction with PPA at 150°C in MW.

The thermal pre-treatment of P25 at 1000°C on the other hand causes the complete rutilation of anatase crystals combined with a dramatic increase of the primary particle size and consequent decrease of surface area[11]. The IR spectrum of P25 TiO_2 pre-treated at 1000°C prior to reaction with PPA at 150°C does not show any absorbance related to $–P(O–Ti)_3$ units, P-C bonds and phenyl

groups (Figure 12B). The ATR-IR data are confirmed by the absence of phosphorous resonance signals in the ^{31}P-NMR spectrum. These data demonstrate that the rutilation and the consequent reduction of the surface area[11] deactivates both the surface grafting and the titaniumphenylphosphonate formation.

CONCLUSION

This study presents a detailed insight regarding the influence of the temperature on the reaction mechanism of the modification of TiO_2 by phenylphosphonic acids (PPA). Reactions were performed in a microwave reactor because it assures a more uniform distribution of the heat and allows to apply temperatures above the boiling point of the solvent. Solid-state ^{31}P-NMR and ATR-FTIR spectroscopy are shown to be useful tools for evaluating the resulting PPA surface modified P25 nanocrystals as well as the titaniumphenylphosphonate formation. It is demonstrated that the formation of titaniumphenylphosphonate starts around 45°C and its amount increases with increasing reaction temperature. At a reaction temperature of 150°C, most of the PPA in the reaction mixture is involved in the formation of titaniumphenylphosphonate. The monitoring of the titaniumphenylphosphonate formation is possible via dedicated signals in the ATR-IR spectrum (around 1023 and 1080 cm^{-1}) and a sharp resonance signal in the ^{31}P SS-NMR spectrum (-4 ppm). Dedicated experiments performed under anhydrous conditions demonstrate that the presence of water is crucial for the formation of titaniumphenylphosphonate. Even at high temperatures, the absence of water results only in the surface grafting of the P25 nanocrystals without any formation of titaniumphenylphosphonate. Investigation of the reactivity of P25 after calcination at 600°C reveals a distinct correlation between the amount of amorphous titanium dioxide and the formation of titaniumphenylphosphonate. In conclusion, this study clearly shows that the modification of P25 is not only affected by the reaction conditions, but that the crystal-amorphous phases composition should also be considered as another key parameter.

ASSOCIATED CONTENT

Supporting information file contains the figures: supporting information 1, supporting information 2, supporting information 3.

AUTHOR INFORMATION

Corresponding Authors:

Email: marco.tassi@uhasselt.be , robert.carleer@uhasselt.be

Author contributions

The manuscript was written through the contributions of all authors. All authors have given approval to the final version of the manuscript.

Notes

The authors declare no competing financial interest.

ACKNOWLEDGMENT

This work is financially supported by the Fund for Scientific Research of Flanders (FWO-Vlaanderen) via the project G.O127.12N. We further acknowledge the financial support from the Interuniversity Attraction Poles Programme (P7/05) initiated by the Belgian Science Policy Office (BELSPO).

REFERENCES

(1) Kango, S.; Kalia, S.; Celli, A.; Njuguna, J.; Habibi, Y.; Kumar, R. Surface Modification of Inorganic Nanoparticles for Development of Organic–inorganic nanocomposites—A Review. *Prog. Polym. Sci.* **2013**, *38* (8), 1232–1261.

(2) Sperling, R. A.; Parak, W. J. Surface Modification, Functionalization and Bioconjugation of Colloidal Inorganic Nanoparticles. *Philos. Trans. R. Soc. Lond. Math. Phys. Eng. Sci.* **2010**, *368* (1915), 1333–1383.

(3) Liu, X.; Chu, P. K.; Ding, C. Surface Modification of Titanium, Titanium Alloys, and Related Materials for Biomedical Applications. *Mater. Sci. Eng. R Rep.* **2004**, *47* (3–4), 49–121.

(4) Yeo, I.-S. Reality of Dental Implant Surface Modification: A Short Literature Review. *Open Biomed. Eng. J.* **2014**, *8*, 114–119.
(5) Rahman, I. A.; Padavettan, V. Synthesis of Silica Nanoparticles by Sol-Gel: Size-Dependent Properties, Surface Modification, and Applications in Silica-Polymer Nanocomposites — a Review. *J Nanomater.* **2012**, *2012*, 8:8–8:8.
(6) Schwartz, J.; Avaltroni, M. J.; Danahy, M. P.; Silverman, B. M.; Hanson, E. L.; Schwarzbauer, J. E.; Midwood, K. S.; Gawalt, E. S. Cell Attachment and Spreading on Metal Implant Materials. *Mater. Sci. Eng. C* **2003**, *23* (3), 395–400.
(7) Gawalt, E. S.; Brault-Rios, K.; Dixon, M. S.; Tang, D. C.; Schwartz, J. Enhanced Bonding of Organometallics to Titanium via a Titanium(III) Phosphate Interface. *Langmuir* **2001**, *17* (21), 6743–6745.
(8) Diebold, U. The Surface Science of Titanium Dioxide. *Surf. Sci. Rep.* **2003**, *48* (5–8), 53–229.
(9) Ohno, T.; Sarukawa, K.; Tokieda, K.; Matsumura, M. Morphology of a TiO2 Photocatalyst (Degussa, P-25) Consisting of Anatase and Rutile Crystalline Phases. *J. Catal.* **2001**, *203* (1), 82–86.
(10) Petru Apopei, C. C. Mixed-Phase TiO2 Photocatalysts: Crystalline Phase Isolation and Reconstruction, Characterization and Photocatalytic Activity in the Oxidation of 4-Chlorophenol from Aqueous Effluents. *Appl. Catal. B Environ.* **2014**, *160-161*, 374–382.
(11) Porter, J. F.; Li, Y.-G.; Chan, C. K. The Effect of Calcination on the Microstructural Characteristics and Photoreactivity of Degussa P-25 TiO2. *J. Mater. Sci.* **1999**, *34* (7), 1523–1531.
(12) Jensen, H.; Pedersen, J. H.; J⊘rgensen, J. E.; Pedersen, J. S.; Joensen, K. D.; Iversen, S. B.; S⊘gaard, E. G. Determination of Size Distributions in Nanosized Powders by TEM, XRD, and SAXS. *J. Exp. Nanosci.* **2006**, *1* (3), 355–373.
(13) Ohtani, B.; Prieto-Mahaney, O. O.; Li, D.; Abe, R. What Is Degussa (Evonik) P25? Crystalline Composition Analysis, Reconstruction from Isolated Pure Particles and Photocatalytic Activity Test. *J. Photochem. Photobiol. Chem.* **2010**, *216* (2–3), 179–182.
(14) David Maria Tobaldi, R. C. P. Fully Quantitative X-Ray Characterisation of Evonik Aeroxide TiO2 P25®. *Mater. Lett.* **2014**, *122*, 345.
(15) Queffélec, C.; Petit, M.; Janvier, P.; Knight, D. A.; Bujoli, B. Surface Modification Using Phosphonic Acids and Esters. *Chem. Rev.* **2012**, *112* (7), 3777–3807.
(16) Ma, T.-Y.; Lin, X.-Z.; Yuan, Z.-Y. Cubic Mesoporous Titanium Phosphonates with Multifunctionality. *Chem. – Eur. J.* **2010**, *16* (28), 8487–8494.
(17) Gao, W.; Dickinson, L.; Grozinger, C.; Morin, F. G.; Reven, L. Self-Assembled Monolayers of Alkylphosphonic Acids on Metal Oxides. *Langmuir* **1996**, *12* (26), 6429–6435.
(18) Raza, M.; Bachinger, A.; Zahn, N.; Kickelbick, G. Interaction and UV-Stability of Various Organic Capping Agents on the Surface of Anatase Nanoparticles. *Materials* **2014**, *7* (4), 2890–2912.
(19) Phillips, M. J.; Duncanson, P.; Wilson, K.; Darr, J. A.; Griffiths, D. V.; Rehman, I. Surface Modification of Bioceramics by Grafting of Tailored Allyl Phosphonic Acid. *Adv. Appl. Ceram.* **2005**, *104* (5), 261–267.
(20) Guerrero, G.; Alauzun, J. G.; Granier, M.; Laurencin, D.; Mutin, P. H. Phosphonate Coupling Molecules for the Control of Surface/interface Properties and the Synthesis of Nanomaterials. *Dalton Trans.* **2013**, *42* (35), 12569–12585.
(21) Souma, H.; Chiba, R.; Hayashi, S. Solid-State NMR Study of Titanium Dioxide Nanoparticles Surface-Modified by Alkylphosphonic Acids. *Bull. Chem. Soc. Jpn.* **2011**, *84* (11), 1267–1275.
(22) Guerrero, G.; Mutin, P. H.; Vioux, A. Anchoring of Phosphonate and Phosphinate Coupling Molecules on Titania Particles. *Chem. Mater.* **2001**, *13* (11), 4367–4373.

(23) Luschtinetz, R.; Frenzel, J.; Milek, T.; Seifert, G. Adsorption of Phosphonic Acid at the TiO2 Anatase (101) and Rutile (110) Surfaces. *J. Phys. Chem. C* **2009**, *113* (14), 5730–5740.
(24) Brodard-Severac, F.; Guerrero, G.; Maquet, J.; Florian, P.; Gervais, C.; Mutin, P. H. High-Field 17O MAS NMR Investigation of Phosphonic Acid Monolayers on Titania. *Chem. Mater.* **2008**, *20* (16), 5191–5196.
(25) Gervais, C.; Profeta, M.; Lafond, V.; Bonhomme, C.; Azaïs, T.; Mutin, H.; Pickard, C. J.; Mauri, F.; Babonneau, F. Combined Ab Initio Computational and Experimental Multinuclear Solid-State Magnetic Resonance Study of Phenylphosphonic Acid. *Magn. Reson. Chem.* **2004**, *42* (5), 445–452.
(26) Adela A Anillo, M. A. V.-G. Textural Properties of Alpha-titanium(IV) Phenylphosphonate: Influence of Preparation Conditions. *Mater. Res. Bull.* **1999**, *34* (4), 627–640.
(27) Jaimez, E.; Bortun, A.; Hix, G. B.; García, J. R.; Rodríguez, J.; Slade, R. C. T. Synthesis of Phosphate–phenylphosphonates of titanium(IV) and Their N-Butylamine Intercalates. *J. Chem. Soc. Dalton Trans.* **1996**, No. 11, 2285–2292.
(28) Pramanik, M.; Patra, A. K.; Bhaumik, A. Self-Assembled Titanium Phosphonate Nanomaterial Having a Mesoscopic Void Space and Its Optoelectronic Application. *Dalton Trans.* **2013**, *42* (14), 5140–5149.
(29) Mutin, P. H.; Guerrero, G.; Vioux, A. Hybrid Materials from Organophosphorus Coupling Molecules. *J. Mater. Chem.* **2005**, *15* (35-36), 3761–3768.
(30) Polshettiwar, V.; Varma, R. S. Aqueous Microwave Chemistry: A Clean and Green Synthetic Tool for Rapid Drug Discovery. *Chem. Soc. Rev.* **2008**, *37* (8), 1546–1557.
(31) Ashley, B.; Lovingood, D. D.; Chiu, Y.-C.; Gao, H.; Owens, J.; Strouse, G. F. Specific Effects in Microwave Chemistry Explored through Reactor Vessel Design, Theory, and Spectroscopy. *Phys. Chem. Chem. Phys.* **2015**, *17* (41), 27317–27327.
(32) Dahal, N.; García, S.; Zhou, J.; Humphrey, S. M. Beneficial Effects of Microwave-Assisted Heating versus Conventional Heating in Noble Metal Nanoparticle Synthesis. *ACS Nano* **2012**, *6* (11), 9433–9446.
(33) Shah, J. J.; Mohanraj, K. Comparison of Conventional and Microwave-Assisted Synthesis of Benzotriazole Derivatives. *Indian J. Pharm. Sci.* **2014**, *76* (1), 46–53.
(34) Sarkar, K.; Yokoi, T.; Tatsumi, T.; Bhaumik, A. Mesoporous Hybrid Zirconium Oxophenylphosphate Synthesized in Absence of Any Structure Directing Agent. *Microporous Mesoporous Mater.* **2008**, *110* (2–3), 405–412.
(35) Nilsing, M.; Lunell, S.; Persson, P.; Ojamäe, L. Phosphonic Acid Adsorption at the TiO2 Anatase (1 0 1) Surface Investigated by Periodic Hybrid HF-DFT Computations. *Surf. Sci.* **2005**, *582* (1–3), 49–60.
(36) Nilsing, M.; Persson, P.; Lunell, S.; Ojamäe, L. Dye-Sensitization of the TiO2 Rutile (110) Surface by Perylene Dyes: Quantum-Chemical Periodic B3LYP Computations. *J. Phys. Chem. C* **2007**, *111* (32), 12116–12123.
(37) Clearfield, A. Recent Advances in Metal Phosphonate Chemistry. *Curr. Opin. Solid State Mater. Sci.* **1996**, *1* (2), 268–278.
(38) Stein Sr., E. W.; Clearfield, A.; Subramanian, M. A. Conductivity of Group IV Metal Sulfophosphonates and a New Class of Interstratified Metal Amine-Sulfophosphonates. *Solid State Ion.* **1996**, *83* (1–2), 113–124.
(39) Clearfield, A.; Demadis, K. *Metal Phosphonate Chemistry: From Synthesis to Applications*; Royal Society of Chemistry, 2011.
(40) Alberti, G.; Casciola, M.; Costantino, U.; Vivani, R. Layered and Pillared metal(IV) Phosphates and Phosphonates. *Adv. Mater.* **1996**, *8* (4), 291–303.
(41) K Joseph Antony Raj; B Viswanathan. Effect of Surface Area, Pore Volume and Particle Size of P25 Titania on the Phase Transformation of Anatase to Rutile. *Indian Journal of Chemistry Vol. 48A, October 2009, 1378-1382*. 2009.